Journal of Hazardous Materials 181 (2010) 526–534

Contents lists available at ScienceDirect

Journal of Hazardous Materials

journal homepage: www.elsevier.com/locate/jhazmat

Scorodite encapsulation by controlled deposition of aluminum phosphate coatings

F. Lagno[a], S.D.F. Rocha[b], S. Chryssoulis[c], G.P. Demopoulos[a,*]

[a] Department of Mining and Materials Engineering, McGill University, 3610 University Street, Montreal, QC, Canada H3A 2B2
[b] Mining Engineering Department, Federal University of Minas Gerais, Belo Horizonte, Brazil
[c] Advanced Mineral Technology Laboratory, UWO Research Park, Ontario, Canada

ARTICLE INFO

Article history:
Received 29 January 2010
Received in revised form 7 May 2010
Accepted 10 May 2010
Available online 16 May 2010

Keywords:
Arsenic
Scorodite
Encapsulation
Stabilization
Supersaturation control
Aluminum phosphate

ABSTRACT

A new stabilization process for scorodite ($FeAsO_4{\cdot}2H_2O$) solids based on the concept of encapsulation by controlled deposition of mineral coatings immune to pH or redox potential variations is described. The stability of the encapsulated scorodite with aluminum phosphates under simulated anoxic and oxic environments is demonstrated. Encapsulation experiments were carried out at 95 °C using 50 g/L scorodite in acidic sulphate solution containing 0.16 mol/L of P(V) with Al(III) to P(V) molar ratio of 1 and precipitation pH of 1.7. The encapsulated particles were characterised by XRD, SEM, TOF-SIMS and TOF-LIMS. The coating was crystalline $AlPO_4{\cdot}1.5H_2O$ ranging in thickness from 2.5 to 3.5 μm. Encapsulation of scorodite particles with hydrated aluminum phosphate appears to be effective in controlling/suppressing the release of arsenic under both oxic and anoxic conditions by more than one order of magnitude.

1. Introduction

Arsenic is a major contaminant in the non-ferrous extractive metallurgical industry and the safe disposal of arsenic wastes constitutes an important environmental issue in many countries including Canada, Chile, Brazil and Japan [1]. Its removal and immobilisation from industrial effluents typically involves neutralisation with lime and coprecipitation with ferric ions [2]. This approach, however, is feasible only for the treatment of low arsenic concentration in aqueous effluents. In the case of arsenic-rich and iron-deficient effluents, such as acid plant effluents, or residues and dusts the production of crystalline scorodite ($FeAsO_4{\cdot}2H_2O$) is preferred instead [3]. Crystallisation of scorodite from chloride and sulphate solutions under atmospheric-pressure conditions and temperatures below the water boiling point has been researched extensively since the supersaturation-controlled approach was developed by Demopoulos and co-workers in the 1990s [4–10]. Some advantages of processing scorodite production are its high arsenic content (~30%) and ease of slurry dewatering.

Scorodite, however, is stable only under oxic and acidic conditions [11–14]. According to a recently completed study [14] the incongruent dissolution of scorodite is very slow, leading to formation of a highly metastable nano-crystalline ferrihydrite phase and simultaneous release of arsenic into solution. The solubility of scorodite at 22 °C was determined to be in the order of 1 mg/L As(V) at pH 6 and 5.8 mg/L As(V) at pH 7. Higher solubility values were observed in the alkaline region [14]. This implies that the disposal of scorodite is environmentally feasible only at pH < 7.

A special issue, related to the stability of scorodite, is its decomposition under anaerobic conditions. Rochette et al. [15], reported that scorodite undergoes reductive break down, when $e_h < 100$ mV at 5.5 < pH < 7 releasing As(III) to groundwater. Similarly, crystalline Fe(III)–As(V) precipitates (basic ferric arsenate sulphate, BFAS [16]), produced in an autoclave (190 °C) and stored in an impounded tailings pond have been found to undergo reductive dissolution releasing As(III) (and Fe(II)) [17]. Typically anaerobic conditions are known to develop in aqueous environments below about 2 m depth [18]. Hence it is of interest to explore means that can render scorodite immune to pH (alkaline) or redox potential (reducing) variations enhancing thereby its stability.

It is the scope of this paper to describe a new stabilization process for scorodite-type solids based on the concept of encapsulation by controlled deposition of mineral coatings resistant to pH or redox alteration. Evangelou [19] has described a similar concept in order to prevent pyrite–pyrrhotite oxidation and acid production in pyritic waste. One of the encapsulation methodologies involved coating pyrite with an iron phosphate layer. In the

* Corresponding author. Tel.: +1 514 398 2046; fax: +1 514 398 4492.
E-mail addresses: george.demopoulos@mcgill.ca (G.P. Demopoulos), sonia.denise@pq.cnpq.br (S.D.F. Rocha).

0304-3894/$ – see front matter © 2010 Elsevier B.V. All rights reserved.
doi:10.1016/j.jhazmat.2010.05.046

present work, an isostructural to scorodite mineral (hydrated aluminum phosphate) was selected as encapsulating material because of its chemical–structural compatibility that allows for heterogeneous nucleation and growth on the surface of scorodite, on one hand, and its resistance to reductive breakdown on the other. This paper, in particular, provides a description of the controlled deposition–encapsulation process and examines the stability of the encapsulated scorodite under simulated anoxic (anaerobic) and oxic (aerobic) environments.

2. Experimental

2.1. Preparation of scorodite

The scorodite substrate material was produced via atmospheric precipitation by the method previously developed at McGill's Hydrometallurgy Laboratory [5,7–8]. The procedure involved placing 1.5 L of isomolar As(V)–Fe(III)–H_2SO_4 ($C_{As} = C_{Fe} = 0.13$ M) solution in a 3 L Applikon reactor equipped with pH, temperature and agitation speed controls. All the reagents and chemicals used were of analytical grade. The solution was heated to 95 °C under stirring and the pH was adjusted to 0.9. Under these conditions the solution is metastable [6]. Upon the addition of hydrothermally prepared scorodite seed [20] precipitation of scorodite was initiated and carried out for at least 2 h. During precipitation the solution pH shifted to lower values but no adjustment was made since according to previous work [8] the arsenic removal efficiency is not significantly affected.

2.2. Heterogeneous deposition–encapsulation

Scorodite solids were repulped and magnetically stirred at pH = 2 for 24 h, in order to remove any amorphous material prior to the encapsulation tests. At the end of each washing step, the slurry was filtered under pressure and the solids were washed by repulping them 3 times with 1000 mL of acidified deionised hot water (pH ~ 3 and 60 °C). The freshly cleaned scorodite particles were subsequently used for encapsulation with aluminum phosphate.

The encapsulation experiments were carried out in the 3 L reactor mentioned in Section 2.1 for times from 1 to 6 h. The reactor was filled with 1.5 L of an acidic sulphate solution containing ~0.16 mol/L of P(V) and a ratio of Al(III) to P(V) of 1:1. The solution was heated to 95 °C and then neutralised with 1 mol/L NaOH, until the precipitation pH of 1.7 was reached. This pH was selected to fall within the metastable zone of aluminum phosphate crystallisation as determined elsewhere [21]. The solution was allowed to stabilize for 30 min in order to assure uniform supersaturated conditions and then 50 g/L of scorodite solids was added to initiate the heterogeneous deposition process; pH was kept constant using NaOH (1 mol/L) as base. Samples of slurry were taken at regular time intervals, filtered through a membrane of 0.22 μm pore size and the filtrate was diluted with acidified (w_{HNO_3} ~5%) deionised water. Nitric acid was used in order to keep the same solution matrix, as the ICP standards are in nitric acid solution.

2.3. Characterisation and analysis

At the end of each test, the entire suspension was filtered. Solids were washed by repulping 3 times with 1000 mL of HCl acidified deionised hot water (60 °C). The calcium, aluminum, iron, arsenic, and phosphorus contents in filtrates and intermediate samples were determined by inductive coupled plasma atomic emission spectrophotometry (ICP-AES). Chemical analysis of solids was done by ICP-AES analysis following their acidic digestion. For X-ray diffraction (XRD) analysis, a Rigaku Rotaflex D-Max diffractometer equipped with a rotative anode and a copper target ($K\alpha_1$ copper with $K\alpha = 0.15406$ nm) was used. The final solids, previously coated with gold, were observed with a JEOL 840A scanning electron microscope (SEM). The size of particles and their mode of distribution were determined using a Horiba LA-920 Laser scattering particle-size distribution analyser.

In addition, secondary electron microscopy analysis and elemental mapping were also obtained using a variable pressure scanning electron microscope (SEM type Hitachi S-3000N). Grains were mounted in epoxy and polished to create grain mounts similar to those used for reflected light microscopy.

Surface composition analysis and depth-profile of the encapsulated scorodite particles were investigated using SEM-EDX (scanning electron microscope equipped with an energy dispersive X-ray analyser), TOF-SIMS (time of flight secondary ion mass spectrometer), and TOF-LIMS (time of flight laser ionisation mass spectrometer). Solids were screened at 40 and 20 μm. For the analysis of particles via TOF-SIMS and TOF-LIMS scorodite particles were randomly selected from the +40 μm fraction and mounted on indium foil. One row of grains was used for each of TOF-SIMS and TOF-LIMS analysis, SEM-EDX, TOF-LIMS and TOF-SIMS.

2.4. Stability testing

Four different materials were studied; the scorodite substrate material itself, scorodite particles coated by one controlled crystallisation–deposition run of $AlPO_4{\cdot}1.5H_2O$ (AlP(1)); scorodite coated with $AlPO_4{\cdot}1.5H_2O$ after one recycle of the coated substrate (AlP(2)); and scorodite after two recycles of the coated substrate (AlP(3)). Two different stability tests were performed under oxic and anoxic conditions. Prior to the stability tests the solids were subjected to a surface cleaning procedure by stirring a 3% solids suspension at the specified pH and room temperature (22 °C) during 24 h in order to ensure that any amorphous material is removed as described elsewhere [14].

2.4.1. Oxic stability test

The stability of the encapsulated scorodite was studied as a function of pH under oxic conditions at room temperature: pH 4.0, 6.0 and 8.0. The slurry was filtered on a 0.1 μm membrane and the solids were washed with pure water using 4 times the volume of filtrate. The solids were immediately repulped to undergo another similar test. The procedure was repeated 3 times. The oxic stability test followed the same methodology as per Bluteau and Demopoulos [14]. The stability test lasted 10 days.

2.4.2. Anoxic stability test

This test was conducted at controlled reducing potential (e_h) conditions (100 ± 20 mV, adjusted twice a day) via addition of 0.5 mol/L NaHS solution. The pH of the solution was monitored and periodically adjusted to pH 7 ± 0.2. For each anoxic stability test, 5% pulp was prepared and the e_h and pH were adjusted as described previously. The anoxic stability test lasted 6 weeks.

For both, anoxic and oxic tests, samples were taken and filtered using 0.25 μm membranes, acidified with 3 drops of concentrated H_2SO_4 solution ($w_{H_2SO_4}$ ~96%) and analysed. The pH was measured using a Ross™ combination electrode with a reported accuracy of ±0.02 pH units (±4.5% in H^+ activities). The e_h was measured using a Cole-Parmer® ORP platinum combination electrode (Ag/AgCl) with a reported accuracy ±20 mV. All experiments were carried out in duplicate runs and performed at room temperature (22 °C).

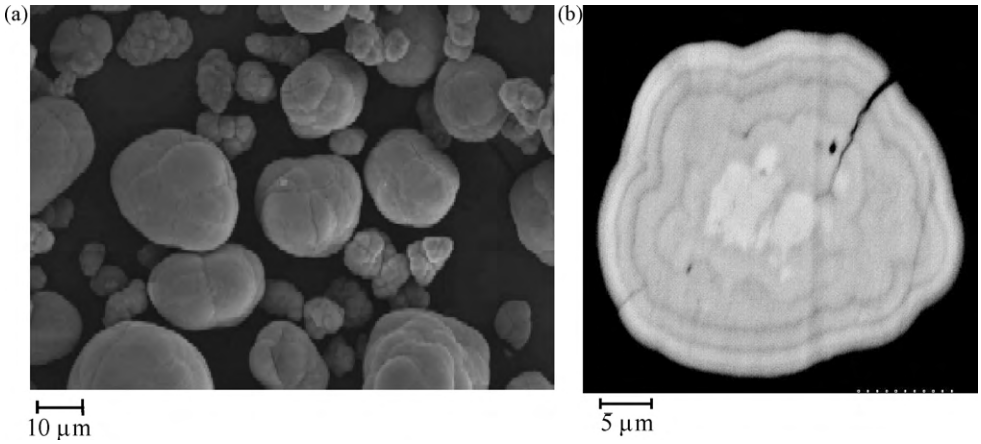

Fig. 1. Scanning electron micrograph of scorodite material used in encapsulation tests: (a) magnification 1000× and (b) magnification 3000×. Backscattered electrons images.

3. Results and discussion

3.1. Scorodite substrate material

XRD analysis (not shown) confirmed the synthetic substrate material used in the encapsulation tests to be scorodite with good crystallinity, as presented in a previous work [14]. Fig. 1 shows SEM and backscattered electron images of the synthetic scorodite. The material consisted of dense agglomerated particles with average size in the order of 25 μm. The scorodite particles are seen to have grown through multiple surface deposition cycles. The lighter core observed in Fig. 1(b) represents the hydrothermal seed used in the preparation of scorodite by atmospheric-pressure precipitation [7].

Chemical composition analysis of the solids confirmed that the material was scorodite. The mass fraction of As and Fe ($w_{As} = 32.4\%$ and $w_{Fe} = 23.6\%$) were in good agreement with the theoretical values of As and Fe in scorodite ($w_{As} = 32.5\%$ and $w_{Fe} = 24.2\%$). A minor amount of SO_4^{2-} (mass fraction of 2.6%) was also found to be incorporated in the scorodite reflecting the fact that synthesis took place in a sulphate-based system [8].

3.2. Aluminum phosphate deposition kinetics

Fig. 2(a) and (b) shows the precipitation kinetics of a typical deposition test in terms of P(V) and Al(III) removal and As(V) and Fe(III) dissolution with time, respectively. The shape of these curves suggests the deposition process to comprise two main stages. The first stage corresponds to an induction period, of approximately 3 h of duration, during which very slow removal of P(V) takes place (with almost no precipitation of Al(III)), accompanied by the release of arsenic (but no iron) from scorodite.

This behaviour can be explained by an "ion exchange"-type process between As(V) and P(V) according to reaction (1):

$$FeAsO_4{\cdot}2H_2O + xH_3PO_{4(aq)} \rightarrow Fe(AsO_4)_{1-x}(PO_4)_x{\cdot}2H_2O + xH_3AsO_{4(aq)} \quad (1)$$

In stage 2, stoichiometric precipitation of aluminum phosphate apparently takes place with no simultaneous dissolution of arsenic:

$$Al^{3+} + 2H_3PO_{4(aq)} + xH_2O \rightarrow AlPO_4{\cdot}xH_2O + 3H^+ \quad (2)$$

Aluminum and phosphorus precipitation proceeds at the same rate indicating the production of stoichiometric aluminum phosphate (1:1). In terms of overall kinetics, around 50% of P(V) was removed from the solution after 6 h (or 3 h if induction period is excluded).

Based on the data of Fig. 2, the molar quantities of aluminum and phosphorus removed along with the quantity of arsenic dissolved over consecutive periods of 1.5 h were calculated. During the first 1.5 h of reaction there were $(3.8 \pm 0.3) \times 10^{-3}$ mol/L and $(6.3 \pm 0.8) \times 10^{-3}$ mol/L of Al(III) and P(V) removed, respectively, whereas the amount of arsenic released during the

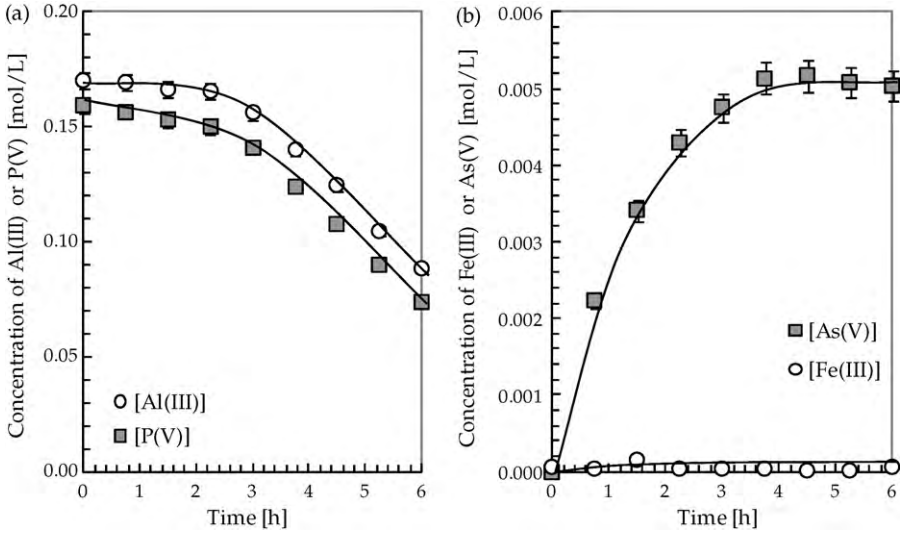

Fig. 2. Controlled deposition of aluminum phosphate on scorodite. (a) Variation of P(V) and Al(III) concentrations with time and (b) variation of As(V) and Fe(III) concentrations with time. Initial P(V) = 0.16 mol/L, Al:P = 1, T = 95 °C, precipitation pH 1.7.

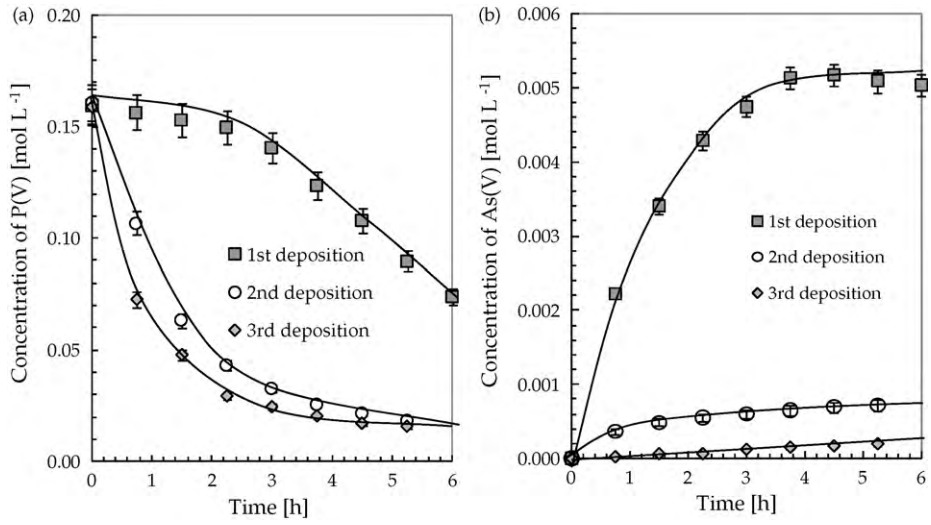

Fig. 3. Controlled crystallisation–deposition of aluminum phosphate on scorodite in three cycles: (a) phosphorus removed from solution and (b) arsenic released into solution as a function of time. Initial P(V) = 0.16 mol/L, Al:P = 1, T = 95 °C, precipitation pH 1.7.

same period was $(3.4 \pm 0.3) \times 10^{-3}$ mol/L. Considering the phase formed is $AlPO_4{\cdot}xH_2O$, this implies that roughly 50% of the phosphate was removed due to aluminum phosphate precipitation and 50% due to ion exchange with arsenate. During the next 1.5 h (1.5–3.0 h), the amount of arsenic released was reduced to $(1.3 \pm 0.1) \times 10^{-3}$ mol/L while the amounts of aluminum and phosphorus precipitated were $(10.0 \pm 2.5) \times 10^{-3}$ mol/L and $(12.3 \pm 1.6) \times 10^{-3}$ mol/L, respectively. In other words, only ~10% of phosphorus removed was due to ion exchange with arsenate. During the subsequent 3–6 h period the release of arsenic was effectively stopped and the removal of aluminum and phosphate proceeded apparently according to the stoichiometry of precipitation reaction (2). Thus, between 3.0 and 4.5 h the ratio of the precipitated aluminum to the precipitated phosphorus was found to be 0.97 ± 0.02 while the same ratio during the last 1.5 h of reaction was 1.07 ± 0.06, i.e. for all practical purposes equal to one.

The growth kinetics of aluminum phosphate deposits on scorodite surface was evaluated carrying out a second and third stage deposition, using the same procedure for the first stage. Fig. 3 shows the kinetics in terms of P(V) precipitation (a), and As(V) release (b). The precipitation rate was faster when the recycled material was used instead of fresh scorodite. In the former, the induction period was effectively eliminated reflecting the faster nucleation kinetics on a surface of similar material, i.e. aluminum phosphate, than on a foreign surface, that is scorodite, $FeAsO_4{\cdot}2H_2O$. As it is seen in Fig. 3(b) the release of arsenic stopped after the second deposition run indicating a complete coverage of scorodite surfaces by aluminum phosphate.

Stoichiometric calculations for the two recycling tests revealed the precipitation of aluminum and phosphorus to have occurred as per reaction (2). Chemical analysis of the products following digestion yielded aluminum to phosphorus molar ratio of 0.96 ± 0.02, 1.04 ± 0.05, and 1.02 ± 0.05 for the first, second and third direct deposition tests, respectively. The (less than one) molar ratio obtained for the solids produced using pure scorodite as substrate confirmed that some phosphorus precipitated via ion exchange (Eq. 1) with arsenic (arsenate) rather than chemical precipitation.

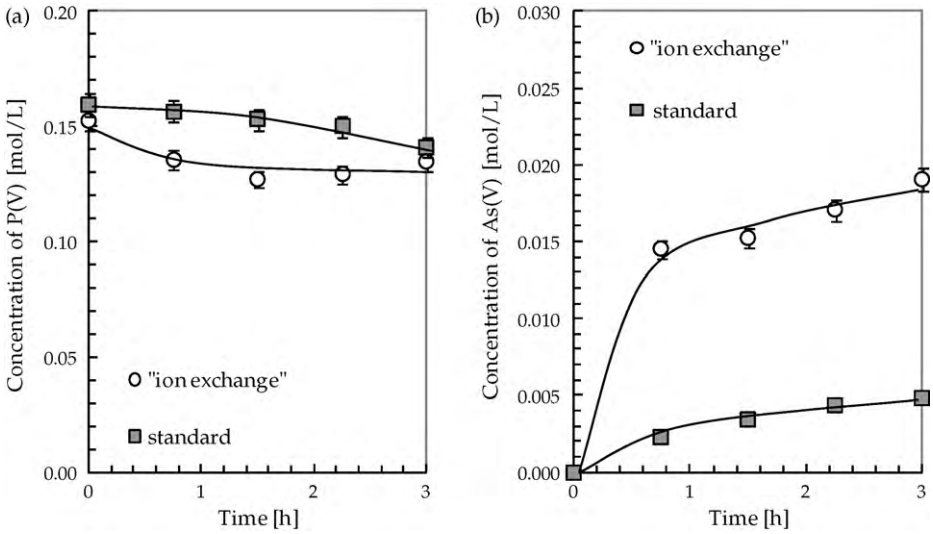

Fig. 4. "Ion exchange" between scorodite and PO_4-containing solution (Al/P ratio = 0) compared to the standard experiment (Al/P ratio = 1). (a) Variation of P(V) removed from solution with time and (b) variation of As(V) released into solution with time. Initial P(V) = 0.16 mol/L, T = 95 °C, precipitation pH 1.7.

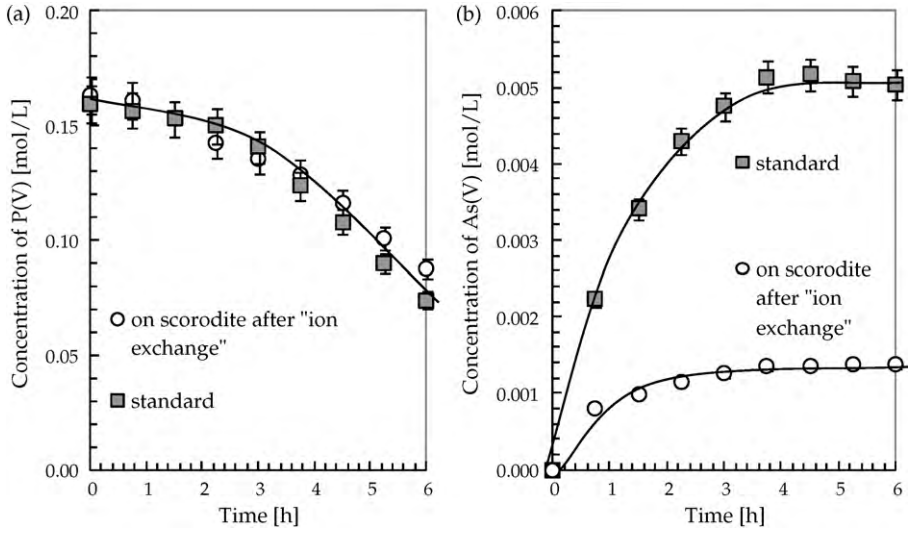

Fig. 5. Deposition of aluminum phosphate on scorodite submitted to "ion exchange" run in comparison to the standard test. (a) Variation of P(V) removed from solution with time and (b) variation of As(V) released into solution with time. Initial P(V) = 0.16 mol/L, Al:P = 1, T = 95 °C, precipitation pH 1.7.

3.3. Heterogeneous nucleation mechanism

As described in the previous section, the deposition of aluminum phosphate on scorodite was preceded by an induction period (~3 h). Based on the analysis of the amounts of P(V) and Al(III) removed and As(V) released, it appears that during this induction period two simultaneous reactions occur: (a) "$PO_4 \leftrightarrow AsO_4$ ion exchange" (Eq. 1) and (b) "$AlPO_4$-precipitation" (Eq. 2).

In order to get a better understanding of this behaviour a number of additional tests was performed. In the first test the postulated "$PO_4 \leftrightarrow AsO_4$ ion exchange" reaction was investigated by removing Al(III) from the system. These tests followed the procedure described in Section 2.2. The variation of the concentration of P(V) and As(V) in solution for this "ion exchange" test (in the absence of Al(III)) is compared to that of a standard test (in the presence of Al(III)) in Fig. 4. The obtained data clearly confirmed the exchange between P(V) (removed from solution) and As(V) (released from scorodite particles). After 3 h of equilibration, the concentration of arsenic in solution was $(19.0 \pm 0.8) \times 10^{-3}$ mol/L as compared to $(17.9 \pm 1.5) \times 10^{-3}$ mol/L of P(V) removed suggesting stoichiometric substitution of phosphate for arsenate as per reaction (1).

Moreover, the release of arsenic was higher than during the course of the direct deposition of aluminum phosphate, $(19.0 \pm 1.5) \times 10^{-3}$ mol/L versus $(4.7 \pm 0.4) \times 10^{-3}$ mol/L of As(V) after 3 h. The difference might be attributed to the effect of Al(III) on free phosphate ion activity. According to Eq. 1 the extent of arsenic release should be proportional to the activity of "H_3PO_4", where "H_3PO_4" encompasses all PO_4 species obtained from the dissociation of orthophosphoric acid. At the pH region (around 1.7) of interest to this work the available species are $H_3PO_4^0$ and $H_2PO_4^-$. On the other hand, when Al(III) is present a number of Al(III)-PO_4 complexes can be formed that effectively lower the activity of free PO_4, i.e. $H_3PO_4^0$ and $H_2PO_4^-$, hence, resulting in decreased release of arsenate.

The solids produced in the "ion exchange" experiment were used as substrate for an aluminum phosphate deposition test using the same experimental conditions as described previously. The results are presented in comparison to standard deposition test in Fig. 5. It can be seen that the same precipitation pattern was obtained following "ion exchange" as in the case of deposition on unreacted scorodite surface. This suggests that the formation of a $Fe(AsO_4)_{1-x}(PO_4)_x \cdot 2H_2O$ surface phase via ion exchange is not the main factor for the heterogeneous nucleation of aluminum phosphate.

3.4. Characterisation of the coating

Fig. 6 shows a backscattered electron (BSE) image of the cross section of a coated scorodite particle along with the associated X-ray elemental maps. This figure clearly shows the aluminum phosphate coating surrounding the original scorodite particle. According to X-ray diffraction analysis performed (not shown), the coated solids had good crystallinity and consisted of a mixture of scorodite and the hydrated aluminum phosphate $H_3(AlPO_4 \cdot 1.5H_2O)$ [21,22]. Backscattered electron micrographs of the solids in different magnifications provided the measurement of the coating width. It was determined that the thickness of the $AlPO_4 \cdot xH_2O$ coating decreases from an average of 3.5 ± 0.2 μm for +40 μm particles, to 3.2 ± 0.4 μm for the fraction (−40 + 20) μm particles and finally to 2.5 ± 0.2 μm for the particles smaller than 20 μm. In several instances it was observed that the $AlPO_4 \cdot xH_2O$ coating was partially detached from the scorodite surface, which apparently was an artifact caused by the drying of the particles prior to screening.

The radial composition of a particle that had lost almost the entire aluminum phosphate layer upon drying and screening was used to better characterise the transition from scorodite to aluminum phosphate (Fig. 7). In the backscattered electron image 12 different white spots are shown and each spot is a burn mark where EDX analysis (Fig. 8) was done. Only the analysis at point #12 represents the aluminum phosphate coating, while analysis at points 9, 10, and 11 appear to represent the phase formed at the very beginning of the deposition process. At the contact zone between the scorodite mantle and Al-phosphate layer (points 9, 10, and 11) there is a clear decrease in all scorodite components (Fe, As) with a simultaneous appearance of sulphur and phosphorus. The phosphorus appearance is believed to be explained by the presence of the surface phase $Fe(AsO_4)_{1-x}(PO_4)_x \cdot 2H_2O$, that was stipulated earlier to form as a result of the ion exchange between AsO_4 and PO_4. Based on the average SEM-EDX analyses from the spots 9, 10, and 11 the following composition was calculated for this phase: $Fe_{0.99}Al_{0.01}H_{0.43}(AsO_4)_{0.94}(PO_4)_{0.15}(SO_4)_{0.08} \cdot xH_2O$ (H^+ is used solely for charge balance purposes). The SEM-EDX analysis also revealed that some of the arsenic, sulphur,

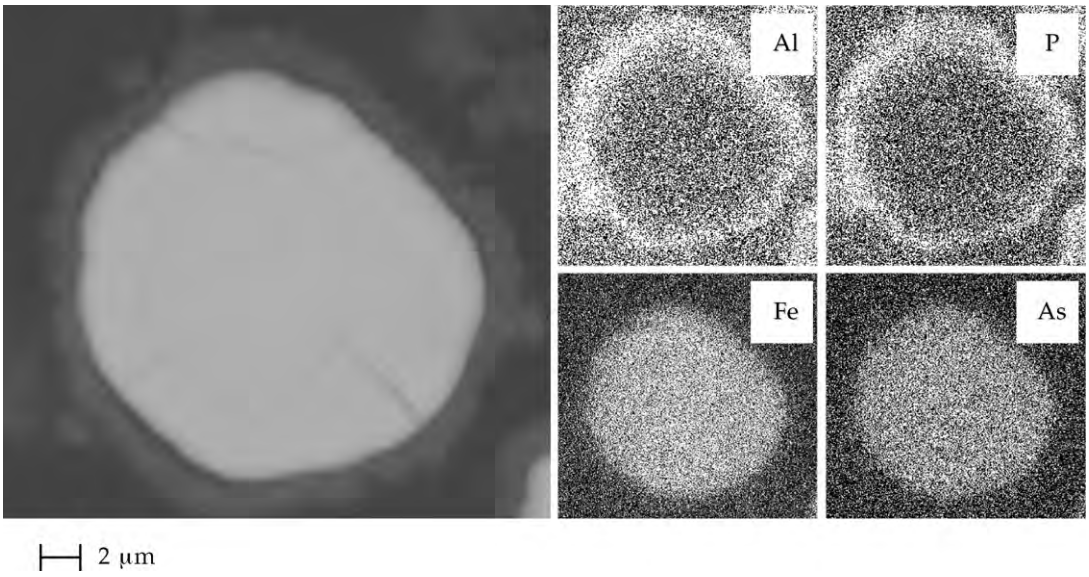

Fig. 6. Backscattered electrons (BSEs) image of a scorodite particle coated with aluminum phosphate material (left) and elemental X-ray maps.

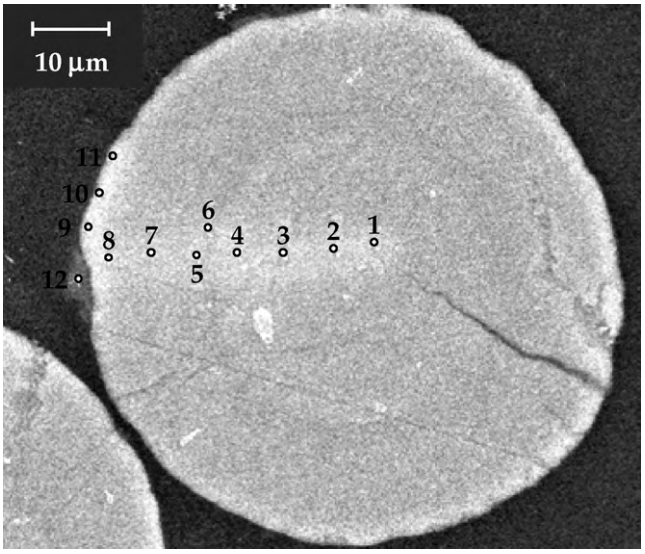

Fig. 7. Backscattered electrons image of a scorodite particle coated with aluminum phosphate material after the bulk of the coating was dislodged.

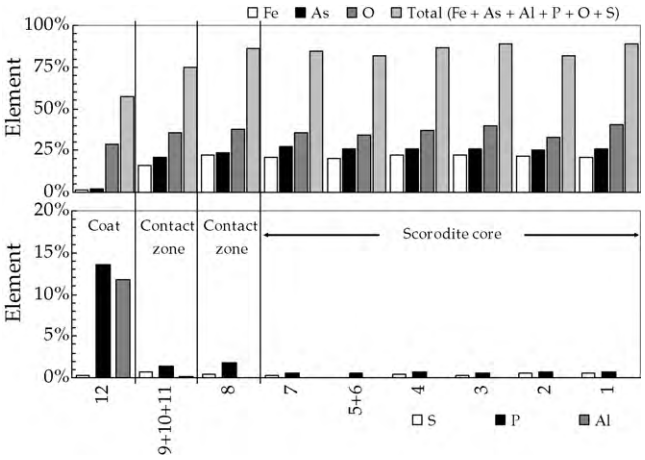

Fig. 8. SEM-EDX radial compositional analysis of coated scorodite particle shown in Fig. 7.

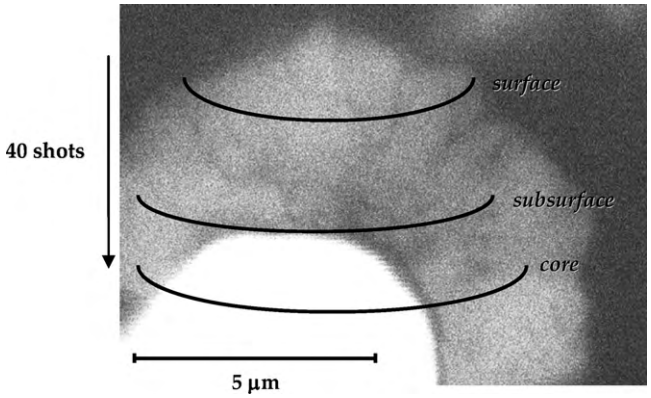

Fig. 9. Depth profiling through the encapsulated scorodite by TOF-LIMS revealing aluminum phosphate coating (surface), aluminum phosphate coating-scorodite interfacial zone (subsurface) and scorodite (core).

and iron were incorporated into the structure of the adjacent aluminum phosphate layer (analysis 12), most likely via substitution. The composition of this layer was estimated to be $Al_{0.93}Fe_{0.07}H_{0.01}(AsO_4)_{0.05}(PO_4)_{0.94}(SO_4)_{0.02}{\cdot}xH_2O$.

The TOF-LIMS spectra collected from the surface region, a subsurface region within the $AlPO_4{\cdot}1.5H_2O$ coating, and from the scorodite core is shown in Fig. 9. The spectra were collected with a sampling depth of <0.1 μm, hence, it took ~40 ablator laser "shots" to reach the scorodite. The analytical results are plotted in Fig. 10. The concentrations are given in arbitrary units (counts in relevant peak over total counts in spectrum). On the left-hand side plot the concentration of positive ions (Al and Fe) is given while on the right-hand side the concentration of negative ions (AsO_4 and PO_4) is shown. More than 20 encapsulated scorodite particles were analysed.

It can be seen from Fig. 10 (left) that the iron concentration is high in the core, intermediate in the subsurface region and low in the surface. Exactly the opposite happens with aluminum. As far as the distribution of phosphate (PO_4) and arsenate (AsO_4) is concerned (Fig. 10 (right)), as expected, the phosphate concentration decreases whereas arsenate concentration increases with depth analysis. However, the analysis shows a significant amount of phosphate present in the core which is believed to be related to the ablation process that resulted in the interference of the coat-

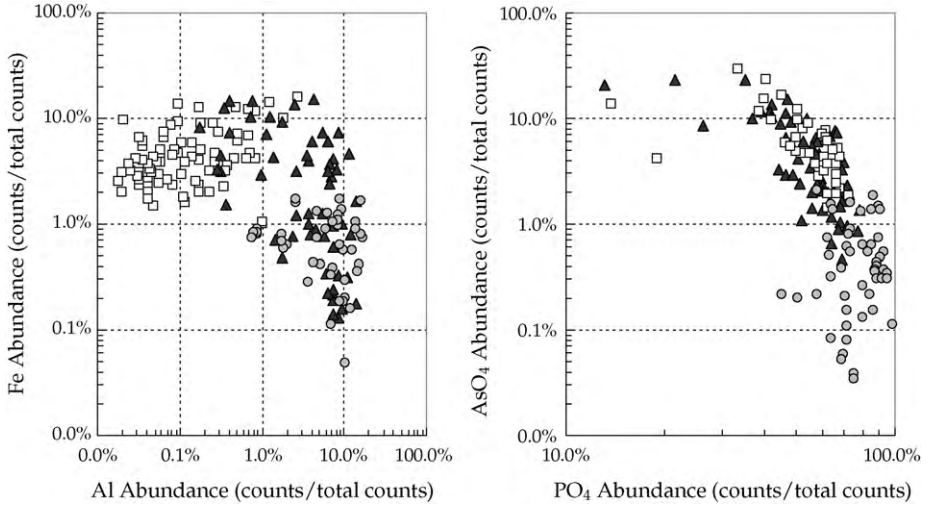

Fig. 10. In depth profiling through $AlPO_4$-coated scorodite. Scatter plot of positive ion (+ve, left) and negative ion (−ve, right). TOF-LIMS data collected at moderate ablator laser energies. Symbols: (□) core; (▲) subsurface; and (●) surface.

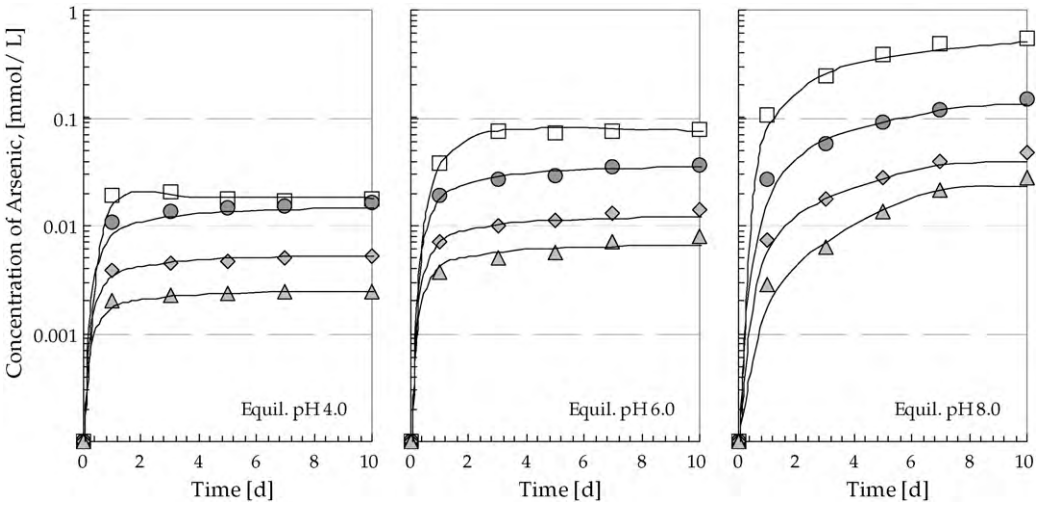

Fig. 11. Dissolution kinetics of arsenic (V) versus time at different equilibration pH under oxic conditions. Symbols: (□) scorodite substrate; (●) AlP(1); (◇) AlP(2); and (△) AlP(3).

ing in the core analysis. The spatial distribution of aluminum and iron (surface/subsurface region versus core) was also verified after various ablation times with the aid of TOF-SIMS (time of flight secondary ion mass spectrometry) (data not shown).

3.5. Stability experiments

3.5.1. Oxic environment

The variation of the solution concentration, in terms of As(V) as a function of time for the experiments performed, is shown in Fig. 11. It is observed that arsenic release was indeed reduced, when the scorodite particles were covered with an aluminum phosphate layer. The release of arsenic was better suppressed, when the solids were coated after two (AlP(2)) and three deposition cycles (AlP(3)). The final arsenic concentration (after 10 days of equilibration) was less by one order of magnitude with the AlP(3) coating than for the uncoated scorodite. In Fig. 12 the final concentrations of P and Al are shown. It is revealed that the dissolution of aluminum phosphate is incongruent in nature according to previous work [23]. However, equilibrium had not been attained after 10 days as the comparison with the solubility data indicates.

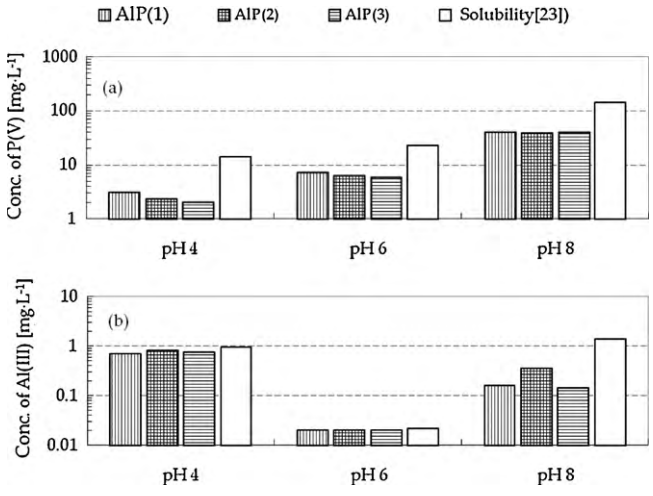

Fig. 12. Concentration of (a) P(V) and (b) Al(III) after 10 days of equilibration compared to solubility of aluminum phosphate.

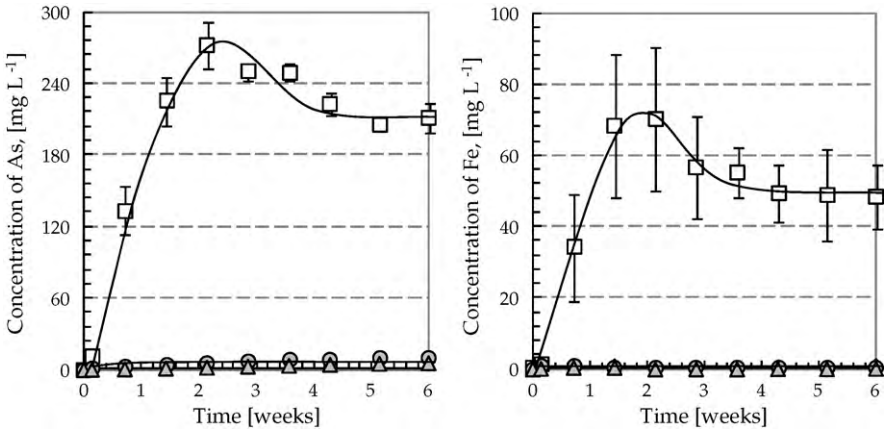

Fig. 13. Dissolution kinetics of total arsenic (left) and total iron (right) versus equilibration time at pH 7 under chemically generated anoxic conditions. Symbols: (□) scorodite substrate; (○) AlP(1); (△) AlP(3).

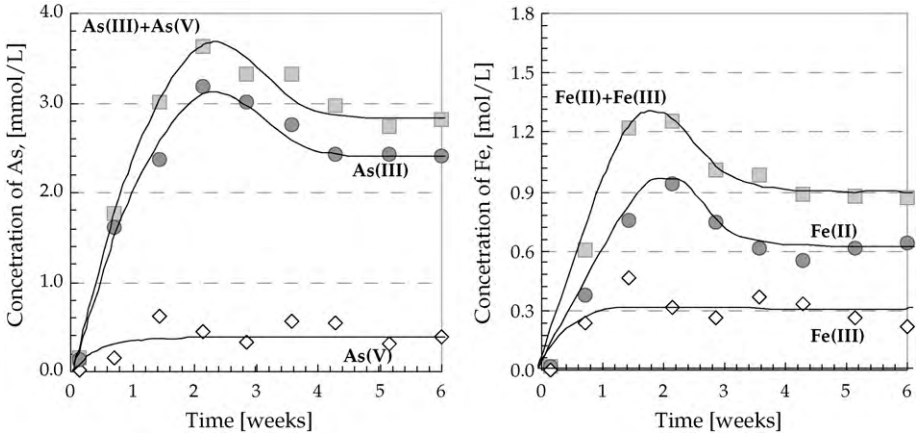

Fig. 14. Dissolution kinetics and speciation of scorodite dissolution at pH 7 under chemically generated anoxic conditions. Arsenic speciation (left); iron speciation (right).

3.5.2. Anoxic environment

Fig. 13 shows that the dissolution kinetics of arsenic and iron were indeed suppressed with the aid of these phosphate coatings. The final concentrations of total iron and total arsenic were reduced, at least, by one order of magnitude. The relatively high "noise" of the concentration data reported is attributed to the lack of precise e_h control. The evolution of iron (ferrous and ferric ions) and arsenic (arsenate and arsenite species) is presented in Fig. 14. It is observed that during the anoxic dissolution of scorodite, the predominant forms of iron and arsenic were Fe(II) and As(III) confirming that scorodite underwent reductive decomposition to Fe(II) and As(III) according to:

$$FeAsO_4{\cdot}2H_2O_{(s)} + 5H^+ + 3e^- \rightarrow Fe^{2+} + H_3AsO_{3(aq)} + 3H_2O \quad (3)$$

Scanning electron micrographs of scorodite particles coated with aluminum phosphate before and after the stability tests showed the coating to remain on the surface of scorodite, confirming the adhesion between the scorodite substrate and the encapsulating aluminum phosphate coating. The dissolution tests indicated the coating does not provide complete sealing of the scorodite surface. Nevertheless, the tests demonstrated that encapsulated scorodite by aluminum phosphate coating releases significantly less arsenic under either oxic or anoxic conditions than unprotected scorodite. The material is hazardous, despite the arsenic to be released to the water during its disposal in landfills will be lower compared to the amount of As released by the uncoated scorodite. However, the environmental impact of the disposal of arsenic as encapsulated scorodite will be decreased.

4. Conclusions

Scorodite was for the first time encapsulated by direct deposition of $AlPO_4{\cdot}1.5H_2O$ ($AlPO_4$-H_3) under controlled supersaturation conditions from a sulphate-matrix solution with Al(III):P(V) molar ratio equal to one at pH 1.7 and 95 °C. The controlled deposition of $AlPO_4{\cdot}1.5H_2O$ on scorodite particles began with an induction period characterised by an "ion exchange" reaction between PO_4 and AsO_4. This "ion exchange" process led to the formation of a solid solution surface layer with the following composition: $Fe_{0.99}Al_{0.01}H_{0.43}(AsO_4)_{0.94}(PO_4)_{0.15}(SO_4)_{0.08}{\cdot}2H_2O$. An investigation of the induction period revealed that the heterogeneous nucleation of $Al_{0.93}Fe_{0.07}H_{0.01}(AsO_4)_{0.05}(PO_4)_{0.94}(SO_4)_{0.02}{\cdot}xH_2O$ is predominant, despite the fact that the "ion exchange" process occurs simultaneously. The induction period was eliminated when $AlPO_4$-coated scorodite particles were recycled. The coating was crystalline $AlPO_4{\cdot}1.5H_2O$ and after one controlled deposition procedure, a uniform in thickness coating, typically ranging from 2.5 to 3.5 μm, was obtained. The coating thickness decreased or increased with the substrate particle size and the number of recycles. The encapsulation of scorodite particles with hydrated aluminum phosphate appears to be effective in partially controlling/suppressing the release of arsenic under both oxic and anoxic conditions. The most interesting results by far are those obtained under the anoxic

stability test since the release of arsenic was decreased by more than one order of magnitude.

Acknowledgments

The support of this work by the Natural Sciences and Engineering Research Council (NSERC) of Canada via a strategic project grant is gratefully acknowledged. The National Council for Scientific and Technological Development (CNPq, Brazil) is also acknowledged.

References

[1] P.A. Riveros, J.E. Dutrizac, P. Spencer, Arsenic disposal practices in the metallurgical industry, Can. Metall. Q. 40 (4) (2001) 395–420.
[2] Y. Jia, G.P. Demopoulos, Coprecipitation of arsenate with iron (III) in aqueous sulfate media: effect of time, lime as base and co-ions on arsenic retention, Water Res. 42 (2008) 661–668.
[3] G.P. Demopoulos, On the preparation and stability of scorodite, in: R.G. Reddy, V. Ramachandran (Eds.), Arsenic Metallurgy, The Minerals, Metals & Materials Society, Warrendale, PA, 2005, pp. 25–50.
[4] G.P. Demopoulos, D. Droppert, G. Van Weert, Precipitation of crystalline scorodite from chloride solutions, Hydrometallurgy 38 (3) (1995) 245–262.
[5] D. Filippou, G.P. Demopoulos, Arsenic immobilization from industrial effluents by controlled scorodite precipitation, JOM 49 (1997) 52–55.
[6] R. Dabekaussen, D. Droppert, G.P. Demopoulos, Ambient pressure hydrometallurgical conversion of arsenic trioxide to crystalline scorodite, CIM Bull. 94 (1051) (2001) 116–122.
[7] S. Singhania, Q. Wang, D. Filippou, G.P. Demopoulos, Temperature and seeding effects on the precipitation of scorodite from sulfate solutions under atmospheric-pressure conditions, Metall. Mater. Trans. B 36B (2005) 327–333.
[8] S. Singhania, Q. Wang, D. Filippou, G.P. Demopoulos, Acidity, valency and third-ion effects on the precipitation of scorodite from mixed sulfate solutions under atmospheric-pressure conditions, Metall. Mater. Trans. B 37B (2006) 189–197.
[9] T. Fujita, R. Taguchi, M. Abumiya, M. Matsumoto, E. Shibata, T. Nakamura, Novel atmospheric scorodite synthesis by oxidation of ferrous sulfate solution, part I, Hydrometallurgy 90 (2–4) (2008) 92–102.
[10] T. Fujita, R. Taguchi, M. Abumiya, M. Matsumoto, E. Shibata, T. Nakamura, Novel atmospheric scorodite synthesis by oxidation of ferrous sulfate solution, part II—effect of temperature and air, Hydrometallurgy 90 (2–4) (2008) 85–91.
[11] E. Krause, V.A. Ettel, Solubility and stability of scorodite. $FeAsO_4{\cdot}2H_2O$: new data and further discussion, Am. Mineral. 73 (1988) 850–854.
[12] D. Langmuir, J. Mahoney, J. Rowson, Solubility products of amorphous ferric arsenate and crystalline scorodite ($FeAsO_4{\cdot}2H_2O$) and their application to arsenic behavior in buried mine tailings, Geochim. Cosmochim. Acta 70 (2006) 2942–2956.
[13] M.C. Harvey, M.E. Schreiber, J.D. Rimstidt, M.M. Griffith, Scorodite dissolution kinetics: implications for arsenic release, Environ. Sci. Technol. 40 (2006) 6709–6714.
[14] M.-C. Bluteau, G.P. Demopoulos, The incongruent dissolution of scorodite: solubility, kinetics and mechanism, Hydrometallurgy 87 (2007) 163–177.
[15] E.A. Rochette, G.C. Li, S.E. Fendorf, Stability of arsenate minerals in soil under biotically generated reducing conditions, Soil Sci. Soc. Am. J. 62 (1998) 1530–1537.
[16] M.A. Gomez, H. Assaaoudi, L. Becze, J.N. Cutler, G.P. Demopoulos, Vibrational spectroscopy study of hydrothermally produced scorodite ($FeAsO_4{\cdot}2H_2O$), ferric arsenate sub-hydrate (FAsH; $FeAsO_4{\cdot}0.75H_2O$) and basic ferric arsenate sulphate (BFAS; $Fe[(AsO_4)_{1-x}(SO_4)_x(OH)_x]{\cdot}wH_2O$), J. Raman Spectrosc. 41 (2010) 212–221.
[17] H. McCreadie, J.L. Jambor, D.W. Blowes, D. Hiller, Geochemical behaviour of autoclave-produced ferric arsenates and jarosite in a gold-mine tailings impoundment, in: W. Petruk (Ed.), Waste Characterization and Treatment, Society for Mining Metallurgy and Exploration, Littleton, CO, 1998, pp. 61–78.
[18] W. Hopkin, The problem of arsenic disposal in non-ferrous metals production, Environ. Geochem. Health 11 (3–4) (1989) 101–112.
[19] V.P. Evangelou, Potential microencapsulation of pyrite by artificial inducement of ferric phosphate coatings, J. Environ. Qual. 24 (3) (1995) 535–542.
[20] J.F. Le Berre, T.C. Cheng, R. Gauvin, G.P. Demopoulos, Hydrothermal synthesis and stability evaluation of mansfieldite in comparison to scorodite, Can. Metall. Q. 46 (2006) 1–10.
[21] F. Lagno, G.P. Demopoulos, Synthesis of hydrated aluminum phosphate, $AlPO_4{\cdot}1.5H_2O$ ($AlPO_4$-H_3), by controlled reactive crystallization in sulfate media, Ind. Eng. Chem. Res. 44 (2005) 8033–8038.
[22] B. Duncan, M. Stocker, D. Gwinup, R. Szostak, K. Vinje, Template-free synthesis of the aluminophosphates H_1 through H_4, Bull. Soc. Chim. France 129 (1992) 98–110.
[23] F. Lagno, G.P. Demopoulos, The dissolution mechanism and solubility of hydrated aluminum phosphate, $AlPO_4{\cdot}1.5H_2O$, Environ. Technol. 27 (2006) 1217–1224.